

INVERSE BREMSSTRAHLUNG CONTRIBUTION TO DRELL–YAN-LIKE PROCESSES

A. B. Arbuzov^{a}, R. R. Sadykov^{b**}*

^a*Bogoliubov Laboratory of Theoretical Physics,
Joint Institute for Nuclear Research
141980, Dubna, Moscow Region, Russia*

^b*Dzheleпов Laboratory of Nuclear Problems,
Joint Institute for Nuclear Research
141980, Dubna, Moscow Region, Russia*

Received August 17, 2007

We consider contribution of the subprocess $\gamma q \rightarrow q' l_1 \bar{l}_2$ in hadron–hadron interactions. It is a part of one-loop electroweak radiative corrections for the Drell–Yan production of lepton pairs at hadron colliders. We show that this contribution must be taken into account aiming at the 1% accuracy of the theoretical description of the Drell–Yan process. Both the neutral and charged current cases are evaluated. Numerical results are presented for typical conditions of LHC experiments.

PACS: 13.40.Ks, 13.85.Qk, 12.15.Lk

1. INTRODUCTION

The Drell–Yan-like processes at high-energy hadron colliders provide an advanced tool for precision studies of several problems in the phenomenology of elementary particles. Studies of single Z and W boson production with the subsequent decays into leptonic pairs play a very important role in the physical programs of the Tevatron [1, 2] and LHC [3, 4]. These processes have large cross sections and clean signatures in the detectors. At the LHC, this allows reaching the 1% experimental accuracy for the total cross sections of these processes as well as high precision in the measurements of differential distributions. In particular, Drell–Yan-like processes are planned to be used at the LHC for luminosity monitoring, W -mass and width measurement, detector calibration, extraction of parton density functions, new physics searches, and other purposes.

Adequately precise theoretical predictions for single Z and W production at the LHC are required. For this reason, we have to scrutinize several effects involved in the derivation of the theoretical accuracy: QCD and electroweak radiative corrections, uncertainties in the

parton density functions, technical precision of Monte Carlo event generators, etc. In this paper, we consider a particular contribution of the first-order electroweak radiative corrections coming from the photon-induced process

$$h_1 + h_2 \rightarrow X + \gamma + q \rightarrow X + q' + l_1 + \bar{l}_2, \quad (1)$$

where $h_{1,2}$ are the initial colliding hadrons, l_1 and \bar{l}_2 is a pair of leptons (e.g., μ^- and μ^+ , or ν_e and e^+), and $X + q'$ denotes the remaining final-state particles (typically, they are hadrons). Here, γ and q are treated as partons found in the initial hadrons with certain energy fractions at a given factorization scale. In this paper, we use the MRST2004QED [5] parameterization of parton density functions, which in particular provides the photon content in proton at the next-to-leading order. We note that the evolution [6] of the parton densities taking the QCD and QED effects into account simultaneously leads to the unique value of the factorization scale, and it is therefore impossible to disentangle the QED and QCD contributions. This leads also to the fact that the reduction of the factorization scale dependence can now be reached only by taking both QED and QCD higher-order radiative corrections into account, which should be done within the same factorization scheme. Nevertheless, due to the smallness of

*E-mail: arbuzov@theor.jinr.ru

**E-mail: srr@nusun.jinr.ru

the fine structure constant α in comparison with the strong coupling constant α_s , we can limit ourselves to the evaluation of only the first-order electroweak corrections [7–16] together with certain higher-order leading logarithmic contributions [17–19]. At the same time, the QCD corrections have to be treated at least at the next-to-next-to-leading order [20–22]. Some numerical results for the inverse bremsstrahlung contribution to the charged current case (single W boson production) were already presented in [23]. We performed an independent calculation and give a comparison with the earlier results below. The neutral current case is considered in addition.

This paper is organized as follows. In the next section, we present the derivation of the Drell–Yan process cross sections in the scheme with massive quarks. The subtraction of the quark mass singularities is described in Sec. 3. Numerical results and their discussion are presented in Sec. 4.

2. INVERSE BREMSSTRAHLUNG WITH MASSIVE QUARKS

We compute the cross section of process (1) in the form proposed by Drell and Yan [24], as a convolution of the parton density functions with the hard subprocess distribution. In our case, the subprocesses are

$$q + \gamma \rightarrow q' + l_1 + \bar{l}_2, \quad (2)$$

where quarks q and q' are of the same type in the neutral current (NC) case and different in the charged current (CC) case. We compute the matrix element of the NC and CC subprocesses with help of the SANC system environment [25, 26]. In the actual calculation, we start with the massive quark scheme. The matching of this scheme with the parton density function formalism is to be performed by means of the subsequent subtraction of the quark mass singularities from the computed cross section. We thus evaluate the complete tree-level matrix elements of the subprocesses in the standard way keeping the exact dependence on the quark and lepton masses. The Feynman diagrams for the subprocesses under consideration are shown in Figs. 1 and 2.

We construct the squares of the matrix elements in the usual way and obtain the parton cross sections of the subprocesses. These quantities then have to be convoluted with the parton density functions:

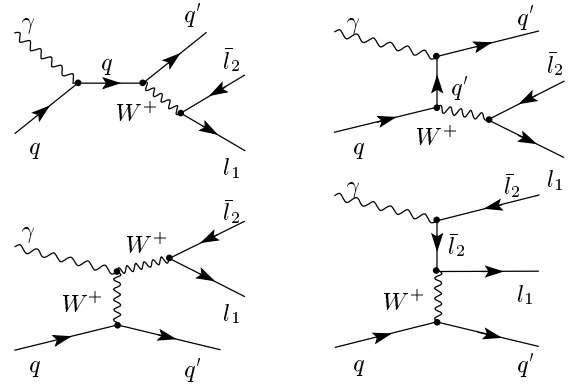


Fig. 1. Feynman diagrams for inverse bremsstrahlung in the charged-current Drell–Yan subprocess

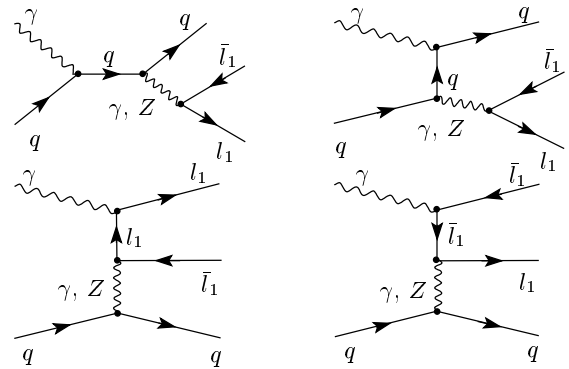


Fig. 2. Feynman diagrams for inverse bremsstrahlung in the neutral current Drell–Yan subprocess

$$\begin{aligned} \frac{d\sigma_{inv\ brems}^{pp \rightarrow l_1 \bar{l}_2 X}(s)}{dc_1} &= \\ &= \sum_{q_i} \int_0^1 \int_0^1 dx_1 dx_2 q_i(x_1, M^2) \gamma(x_2, M^2) \times \\ &\quad \times \frac{d\hat{\sigma}^{q_i \gamma \rightarrow q' l_1 \bar{l}_2}(\hat{s})}{d\hat{c}_1} \mathcal{J} \Theta(c_1, x_1, x_2), \quad (3) \end{aligned}$$

where c_1 denotes the cosine of the scattering angle of the first lepton (another variable can be chosen as well). The step function $\Theta(c_1, x_1, x_2)$ defines the phase-space domain corresponding to the given event selection procedure. The parton cross section is taken in the center-of-mass reference frame of the initial partons, where the cosine of the first lepton scattering angle, \hat{c}_1 , is defined. Passing to the observable variable c_1 involves the

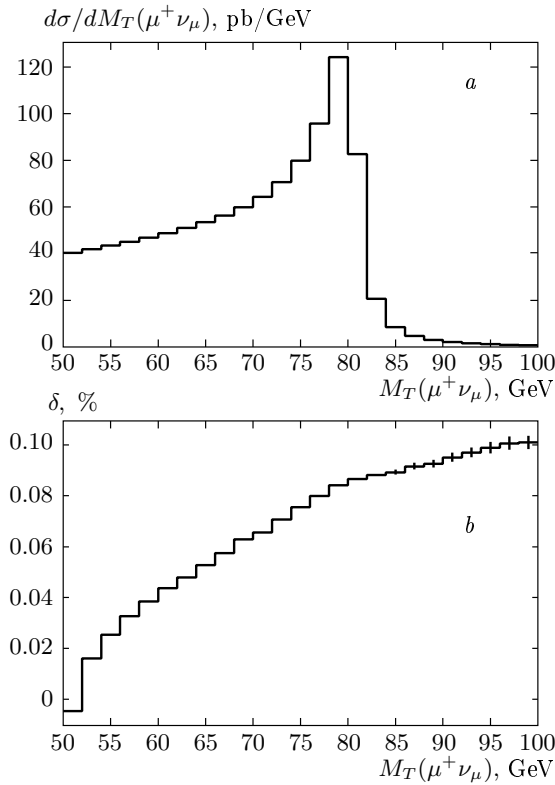


Fig. 3. The Born-level CC Drell-Yan cross section (a) and the relative contribution of the inverse bremsstrahlung (b) versus the transverse mass of the muon-neutrino pair

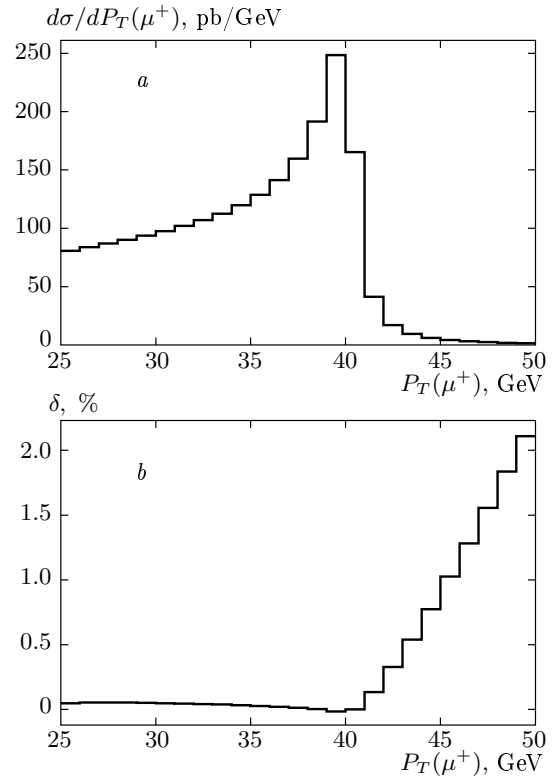


Fig. 4. The Born-level CC Drell-Yan cross section (a) and the relative contribution of the inverse bremsstrahlung (b) versus the μ^+ transverse momentum

Jacobian

$$\mathcal{J} = \frac{\partial \hat{c}}{\partial c} = \frac{4x_1x_2}{a^2}, \quad a = x_1 + x_2 - c(x_1 - x_2), \quad (4)$$

$$\hat{c} = 1 - (1 - c) \frac{2x_1}{a}, \quad \hat{s} = sx_1x_2,$$

where s is the squared center-of-mass energy of the colliding hadrons. An analogous formula can be written for any other choice of a differential distribution and for the total cross section.

In Eq. (3), we presented the contribution in the case where the photon is found in the first of the colliding hadrons and the quark is taken from the other one. Of course, there is also the contribution with the opposite choice of the particles, and it is taken into account in our numerical simulations.

3. SUBTRACTION OF THE QUARK MASS SINGULARITIES

Because the calculation of the parton cross sections was performed keeping the quark masses finite, the re-

sult in (3) depends on the values of the masses. For high energies, this dependence arises in the form of large logarithms of the type of $\ln(M^2/m_q^2)$, which give a considerable numerical effect, while the other mass-dependent contributions are suppressed by the factor $m_q^2/M^2 \ll 1$ and can be omitted (here, M is a typical energy scale of the parton subprocess). The large logarithms represent quark mass singularities. They can be treated with help of the QED renormalization-group approach. But they have already been taken into account in the evolution of the parton density functions. In the MRST2004QED distributions [5], this has been done explicitly. But even in any other available parton density function, the QED evolution is implicitly taken into account because it has not been subtracted from the experimental data before the parton density function fitting procedure. In fact, QED corrections to the quark line in deep inelastic scattering are usually omitted in the data analysis (see Refs. [27, 28]).

The quark mass singularity of the first type arises from the right-hand Feynman diagrams in the upper parts of Figs. 1 and 2 for CC and NC cases, respec-

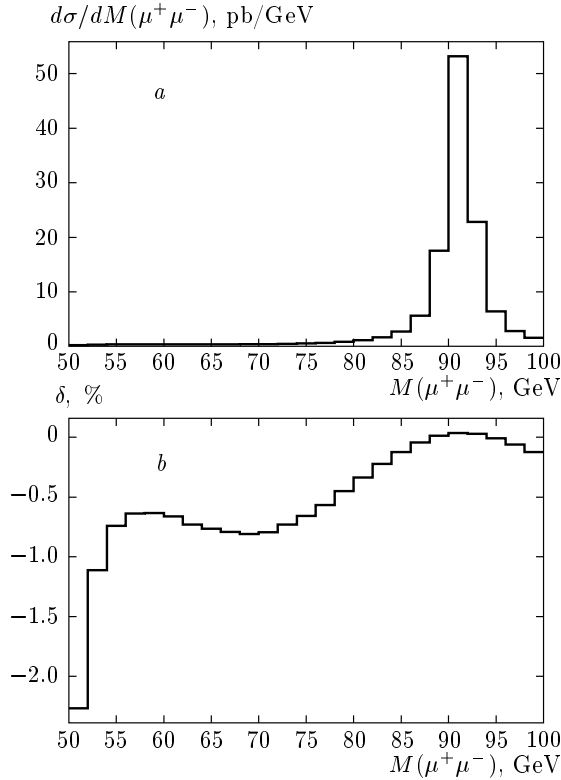


Fig. 5. The Born-level NC Drell-Yan cross section (a) and the relative contribution of the inverse bremsstrahlung (b) versus the invariant mass of the muon pair

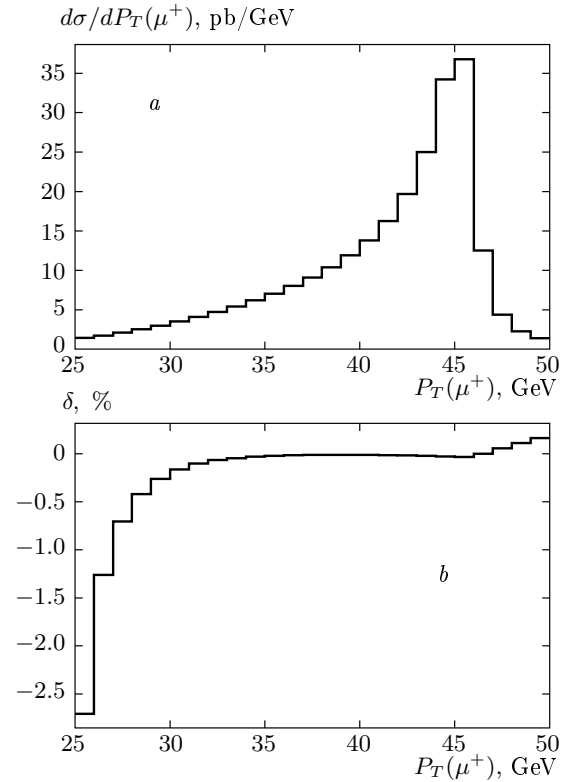


Fig. 6. The Born-level NC Drell-Yan cross section (a) and the relative contribution of the inverse bremsstrahlung (b) versus the μ^+ transverse momentum

tively. The singularity originates from the kinematical domain where the virtual quark propagator is close to the mass shell. For this situation, there is a convolution of distributions of two subprocesses: conversion of the photon into a pair of quarks and the Drell-Yan parton process

$$q'q \rightarrow l_1\bar{l}_2.$$

In the \overline{MS} factorization QED scheme, which is defined in the same way as the QCD one [29], the corresponding contribution is given by

$$\delta_1(c_1) = \sum_{q_i} \int_0^1 \int_0^1 dx_1 dx_2 \gamma(x_1, M^2) q_i(x_2, M^2) \times \\ \times \int_0^1 dx_3 D_{q'\gamma}(x_3, M, m_{q'}) \frac{d\tilde{\sigma}_{q_i q_i \rightarrow l_1 \bar{l}_2}(\tilde{s})}{d\tilde{c}_1} \times \\ \times \tilde{J} \Theta(c_1, x_1 x_3, x_2), \quad (5)$$

where \tilde{c}_1 , \tilde{J} , and \tilde{s} are calculated in accordance with Eq. (4) with the replacement $x_1 \rightarrow x_1 x_3$. In the NC

case, we have $q' = q$ in the above equation. The structure function $D_{q'\gamma}(x_3, M, m_{q'})$ describes the probability to find a quark q' with the energy fraction x_3 in the photon. For the \overline{MS} scheme at the next-to-leading order, this function is given by

$$D_{q'\gamma}^{\overline{MS}}(x_3, M, m_{q'}) = \frac{\alpha}{2\pi} Q_{q'}^2 \ln \frac{M^2}{m_{q'}^2} [x_3^2 + (1-x_3)^2], \quad (6)$$

where M is the factorization scale and $Q_{q'}$ is the quark charge.

In the NC case, there is one additional source of the quark mass singularities. It arises from the two lower Feynman amplitudes in Fig. 2, when the virtual photon propagator is near the mass shell. In this case, we have the convolution of the distributions of the processes:

$$2\gamma \rightarrow l_1 \bar{l}_1 \quad \text{and} \quad q \rightarrow \gamma q.$$

The corresponding contribution is

Table 1. Cross sections σ_0 and $\sigma_{\gamma q}$ of the respective processes $p[q]p[q'] \rightarrow \nu_\mu \mu^+ X$ and $p[\gamma]p[q] \rightarrow \nu_\mu \mu^+ X$ and the corresponding corrections $\delta_{\gamma q} = \sigma_{\gamma q}/\sigma_0$ obtained by DK and SANC groups for different $P_{T,\mu}$ ranges at the LHC

$P_{T,\mu}$, GeV	25 – ∞	50 – ∞	100 – ∞	200 – ∞	500 – ∞	1000 – ∞
σ_0 , pb						
DK	2112.2(1)	13.152(2)	0.9452(1)	0.11511(2)	0.0054816(3)	0.00026212(1)
SANC	2112.2(1)	13.151(1)	0.9451(1)	0.11511(1)	0.0054813(1)	0.00026211(1)
$\delta_{\gamma q}$, %						
DK	0.071(1)	5.24(1)	13.10(1)	16.44(2)	14.30(1)	11.89(1)
SANC	0.074(1)	5.24(1)	13.09(1)	16.43(1)	14.30(1)	11.90(1)

$$\delta_2(c_1) = \sum_{q_i} \int_0^1 \int_0^1 dx_1 dx_2 q_i(x_1, M^2) \gamma(x_2, M^2) \times$$

$$\times \int_0^1 dx_3 D_{\gamma q}(x_3, M, m_q) \frac{d\tilde{\sigma}^{\gamma\gamma \rightarrow l_1 \bar{l}_1}(\tilde{s})}{d\tilde{c}_1} \times$$

$$\times \tilde{J} \Theta(c_1, x_1 x_3, x_2). \quad (7)$$

The relevant structure function describes the probability to find a photon with a certain energy fraction in the quark:

$$D_{\gamma q}^{\overline{MS}}(x_3, M, m_q) = \frac{\alpha}{2\pi} Q_q^2 \frac{1 + (1 - x_3)^2}{x_3} \times$$

$$\times \left\{ \ln \frac{M^2}{m_q^2} - 2 \ln x_3 - 1 \right\}. \quad (8)$$

In accordance with the renormalization formalism, we now have to subtract contributions (5) and (7) from the cross section computed in (3). In a realistic situation, we have to perform this procedure numerically in order to keep the possibility to impose experimental cuts. On the other hand, it can be shown analytically that the terms with the logarithms of the quark masses cancel during the subtraction procedure.

4. NUMERICAL RESULTS AND CONCLUSIONS

For the numerical evaluations, we used the same conditions and the input parameters as in Ref. [23]:

$$G_F = 1.16637 \cdot 10^{-5} \text{ GeV}^{-2},$$

$$\alpha(0) = 1/137.03599911, \quad \alpha_s = 0.1187,$$

$$M_W = 80.425 \text{ GeV}, \quad \Gamma_W = 2.124 \text{ GeV},$$

$$M_Z = 91.1867 \text{ GeV}, \quad \Gamma_Z = 2.4952 \text{ GeV},$$

$$M_H = 150 \text{ GeV}, \quad m_t = 174.17 \text{ GeV},$$

$$m_u = m_d = 66 \text{ MeV}, \quad m_c = 1.55 \text{ GeV},$$

$$m_s = 150 \text{ MeV}, \quad m_b = 4.5 \text{ GeV},$$

$$|V_{ud}| = |V_{cs}| = 0.975, \quad |V_{us}| = |V_{cd}| = 0.222.$$

The MRST2004QED set [5] of parton density functions and the G_F electroweak renormalization scheme [30] were used. The cut on the charged lepton rapidity and transverse momentum are $|\eta_\ell| < 1.2$ and $P_{T,\ell} > 25 \text{ GeV}$. The cut on the missing transverse momentum for the CC case is also imposed: $P_{T \text{ missing}} > 25 \text{ GeV}$.

At the parton level for the CC and NC processes,

$$\gamma + q \rightarrow q' + l_1 + \bar{l}_2,$$

we performed a comparison with the corresponding distributions obtained with help of the CompHEP system [31] and found a good agreement.

In Table 1, we present the results of comparison for the inverse bremsstrahlung contribution to the CC Drell–Yan process with different cuts on the charged lepton transverse momentum (see the details in Ref. [23]). Our results are marked as SANC, they are compared with the numbers (DK) presented in Ref. [23]. The small deviations in the results for the values of the corrections are certainly beyond the 1% precision level. They are due to some differences in the schemes of calculations and are induced by higher-order effects in α .

Table 2 shows the results of comparison for the inverse bremsstrahlung contribution to the CC Drell–Yan

Table 2. Cross sections σ_0 and $\sigma_{\gamma q}$ of the respective processes $p[q]p[q'] \rightarrow \nu_\mu\mu^+X$ and $p[\gamma]p[q] \rightarrow \nu_\mu\mu^+X$ and the corresponding corrections $\delta_{\gamma q} = \sigma_{\gamma q}/\sigma_0$ obtained by DK and SANC groups for different $M_{T,\nu_\mu\mu^+}$ ranges at the LHC

$M_{T,\nu_\mu\mu^+}$, GeV	50 – ∞	100 – ∞	200 – ∞	500 – ∞	1000 – ∞	2000 – ∞
σ_0 , pb						
DK	2112.2(1)	13.152(2)	0.9452(1)	0.057730(5)	0.0054816(3)	0.00026212(1)
SANC	2112.2(1)	13.151(1)	0.9451(1)	0.057730(5)	0.0054813(1)	0.00026211(1)
$\delta_{\gamma q}$, %						
DK	0.0567(3)	0.1347(1)	0.2546(1)	0.3333(1)	0.3267(1)	0.3126(1)
SANC	0.0532(1)	0.1350(1)	0.2537(1)	0.3314(1)	0.3245(1)	0.3094(1)

Table 3. Cross sections σ_0 and $\sigma_{\gamma q}$ of the respective processes $p[q]p[q'] \rightarrow \mu^+\mu^-X$ and $p[\gamma]p[q] \rightarrow \mu^+\mu^-X$ and the corresponding corrections $\delta_{\gamma q} = \sigma_{\gamma q}/\sigma_0$ for different $M_{\mu^+\mu^-}$ ranges at the LHC

$M_{\mu^+\mu^-}$, GeV	50 – ∞	100 – ∞	200 – ∞	500 – ∞	1000 – ∞	2000 – ∞
σ_0 , pb						
HORACE	254.64(1)	10.571(1)	0.45303(3)	0.026996(2)	0.0027130(2)	0.00015525(1)
SANC	254.65(2)	10.571(1)	0.45308(3)	0.026996(2)	0.0027131(2)	0.00015525(1)
$\delta_{\gamma q}$, %						
SANC	0.047(1)	0.449(1)	0.013(1)	0.496(1)	0.619(1)	0.563(1)

process with different cuts on transverse mass of the muon–neutrino pair. The corresponding numbers for $\delta_{\gamma q}$ are below the one-percent level.

Table 3 gives the results for the inverse bremsstrahlung contribution to the NC Drell–Yan process with production of two muons. Different values of the cut on the invariant mass of the muon pair are considered. For the Born cross section, we also show the numbers of HORACE [17, 19], which are in good agreement with the SANC results.

In Fig. 3, we plot the distributions of the Born-level cross section and of the relative radiative correction versus the transverse mass of the muon and neutrino pair $M_T(\mu^+\nu_\mu)$ in the CC Drell–Yan process,

$$M_T(\mu^+\nu_\mu) = \sqrt{2P_{T,\mu}P_{T,\nu}(1 - \cos\phi_{\mu\nu})}, \quad (9)$$

where $\phi_{\mu\nu}$ is the angle between the muon momentum and the missing momentum in the transverse plane. In Fig. 4, analogous distributions in the muon transverse momentum $P_{T,\mu}$ are given.

Figure 5 shows the Born differential cross section of the NC Drell–Yan process and the relative correction

$\delta_{\gamma q}$ as a function of invariant mass $M_{\mu^+\mu^-}$ of the muon pair. Figure 6 gives us results for the Born differential cross section of the neutral current Drell–Yan process and the relative correction $\delta_{\gamma q}$ as a function of the μ^+ transverse momentum $P_{T,\mu}$. The distributions around the W and Z resonances are plotted. The drop-offs in the first bins of the correction distributions in the NC have no physical sense. They arise because the factorization procedure with the longitudinal parton density functions does not allow applying the experimental cuts unambiguously. The drop-offs can be shifted by choosing a different cut value. We checked that the rest of the distributions does not suffer from this problem.

Thus, we presented the photon-induced contribution to the first-order electroweak radiative corrections to Drell–Yan processes. In the case of charged-current scattering, our results are in good agreement with earlier calculations of other groups. The NC case was considered in an analogous manner. This inverse bremsstrahlung contribution should be taken into account together with all other relevant effects to reach the accuracy of the theoretical description of the Drell–Yan process adequate to the precision of

the forthcoming LHC experiments. The typical size of the contribution is below one percent, but for the transverse momentum distribution in CC scattering, the effect can reach up to 16% depending on the cut value. We plan to implement the results of our calculations into a general Monte Carlo event generator for Drell–Yan processes, which is under development in the SANC group.

We are grateful to D. Bardin, S. Bondarenko, P. Christova, and L. Kalinovskaya for fruitful discussions and critical reading of the manuscript. This work was supported by the RFBR (grant № 07-02-00932). One of us (A. A.) also thanks the grant of the RF President (Scientific Schools 5332.2006) and the INTAS (grant № 03-51-2007).

REFERENCES

1. V. M. Abazov et al. [CDF Collaboration], *Phys. Rev. D* **70**, 092008 (2004).
2. S. Abachi et al. [D0 Collaboration], *Phys. Rev. Lett.* **77**, 3309 (1996).
3. G. Altarelli and M. L. Mangano, *Standard Model Physics (and more) at the LHC*, Workshop Proceedings, CERN Report 2000-04, p. 117.
4. N. V. Krasnikov and V. A. Matveev, *Phys. Part. Nucl.* **28**, 441 (1997); and references therein.
5. A. D. Martin, R. G. Roberts, W. J. Stirling, and R. S. Thorne, *Eur. Phys. J. C* **39**, 155 (2005).
6. M. Roth and S. Weinzierl, *Phys. Lett. B* **590**, 190 (2004).
7. V. A. Mosolov and N. M. Shumeiko, *Nucl. Phys. B* **186**, 397 (1981).
8. A. V. Soroko and N. M. Shumeiko, *Sov. J. Nucl. Phys.* **52**, 329 (1990).
9. D. Wackerth and W. Hollik, *Phys. Rev. D* **55**, 6788 (1997).
10. U. Baur, S. Keller, and D. Wackerth, *Phys. Rev. D* **59**, 013002 (1999).
11. S. Dittmaier and M. Krämer, *Phys. Rev. D* **65**, 073007 (2002).
12. U. Baur, O. Brein, W. Hollik, C. Schappacher, and D. Wackerth, *Phys. Rev. D* **65**, 033007 (2002).
13. U. Baur and D. Wackerth, *Phys. Rev. D* **70**, 073015 (2004).
14. C. M. Carloni Calame, G. Montagna, O. Nicrosini, and A. Vicini, *JHEP* **0612**, 016 (2006).
15. V. A. Zykunov, *Phys. Atom. Nucl.* **69**, 1522 (2006).
16. A. Arbuzov, D. Bardin, S. Bondarenko, P. Christova, L. Kalinovskaya, G. Nanava, and R. Sadykov, *Eur. Phys. J. C* **46**, 407 (2006).
17. C. M. Carloni Calame, G. Montagna, O. Nicrosini, and M. Treccani, *Phys. Rev. D* **69**, 037301 (2004).
18. C. M. Carloni Calame, G. Montagna, O. Nicrosini, and M. Treccani, *Eur. Phys. J. C* **33**, S665 (2004).
19. C. M. Carloni Calame, G. Montagna, O. Nicrosini, and M. Treccani, *JHEP* **0505**, 019 (2005).
20. C. Anastasiou, L. J. Dixon, K. Melnikov, and F. Petriello, *Phys. Rev. Lett.* **91**, 182002 (2003).
21. C. Anastasiou, L. J. Dixon, K. Melnikov, and F. Petriello, *Phys. Rev. D* **69**, 094008 (2004).
22. K. Melnikov and F. Petriello, *Phys. Rev. D* **74**, 114017 (2006).
23. C. Buttar et al., E-print archives, hep-ph/0604120.
24. S. D. Drell and T. M. Yan, *Phys. Rev. Lett.* **25**, 316 (1970); *Erratum ibid* **25**, 902 (1970).
25. A. Andonov, A. Arbuzov, D. Bardin, S. Bondarenko, P. Christova, L. Kalinovskaya, G. Nanava, and W. von Schlippe, *Comp. Phys. Comm.* **174**, 481 (2006); *Erratum ibid* doi:10.1016/j.cpc.2007.06.010; and references therein.
26. D. Bardin, S. Bondarenko, L. Kalinovskaya, G. Nanava, L. Rumyantsev, and W. von Schlippe, E-print archives, hep-ph/0506120; submitted to *Comp. Phys. Commun.*
27. A. A. Akhundov, D. Y. Bardin, L. Kalinovskaya, and T. Riemann, *Fortsch. Phys.* **44**, 373 (1996).
28. A. Arbuzov, D. Y. Bardin, J. Bluemlein, L. Kalinovskaya, and T. Riemann, *Comp. Phys. Comm.* **94**, 128 (1996).
29. W. A. Bardeen, A. J. Buras, D. W. Duke, and T. Muta, *Phys. Rev. D* **18**, 3998 (1978).
30. W. Hollik and H. J. Timme, *Z. Phys. C* **33**, 125 (1986).
31. E. Boos et al. [CompHEP Collaboration], *Nucl. Instrum. Meth. A* **534**, 250 (2004).